

# Fabrication of Aluminium Internally Cooled Cutting Tool by Means of Selective Laser Melting (SLM)

*Mohd Hafizu Zakaria*

*Institute of Postgraduate Studies, Universiti Malaysia Pahang,  
Lebuhraya Tun Razak, 26300 Gambang, Kuantan, Pahang, Malaysia*

*Saiful Anwar Che Ghani*

*Wan Sharuzi Wan Harun*

*Zuriadi Zaulkafilai*

*Siti Rohaida Mohamed*

*Human Engineering Group,*

*Faculty of Mechanical Engineering, Universiti Malaysia Pahang,  
26600 Pekan, Pahang, Malaysia*

## ABSTRACT

*A study of aluminium internally cooled cutting tool (ICCT) fabrication by means of selective laser melting is presented, including mechanical property's characterization and physical accuracy considerations. Mechanical performance is first performed on samples with simple geometry to determine density and mechanical strength using aluminium powders. SLM parameters such as laser scanning velocity, laser power and scanning strategy used are default from a machine manufacturer. Physical tests on the actual internal channel of an innovative internally cooled cutting tool such as a channel dimensional accuracy and surface roughness measurement are performed to define quality of the internal cooling channel affected by default process parameters with negligible microstructural defects. The internally cooled cutting tool is then tested in machining mild steel with recommended finishing cutting parameters to confirm its functional integrity and performance.*

**Keywords:** *Internally Cooled Cutting Tool, Additive Manufacturing, Selective Laser Melting, Dimensional Accuracy*

## **Introduction**

Technological progress towards green cutting by adopting dry machining [1], near dry machining [2], and indirect cooling [3] has led towards the application of internally cooled cutting tool [4]. The major factor hampering the development of internally cooled cutting tool is the management of heat transferred into the cutting insert [5, 6]. The high localised heat generated at the rake face of the cutting insert must be channelled away from the vicinity of the cutting zone to ensure the extended useful life of the insert may be achieved and thermal expansion of the workpiece can be avoided.

Nowadays, additive manufacturing (AM) technologies are attracting the attention of designers, researchers and industrial sectors. Additive manufacturing, such as electron beam melting (EBM), direct metal laser sintering (DMLS) and selective laser melting (SLM), is a process that is capable to make complex three-dimensional (3D) metal parts directly from computer-aided design (CAD) by adopting layer-by-layer processing of metal powders. These technologies are customarily utilised to manufacture complex and customised structures that cannot be accomplished economically using conventional manufacturing methods such as machining, sand casting or moulding. SLM offers advantages for parts manufacturing from powder metallurgy in terms of reducing the human resources, raw materials, time, and energy.

Aluminium alloys are utilised as a part of various industrial areas including medical [7], automotive [8], and aerospace [9]. Processing aluminium alloys by SLM is not as easy as with the other materials due to the combination of physical properties such as powder particle size and melting point. Aluminium alloys have high reflectivity and thermal conductivity that convolute a process and contribute in producing porosity in the produced parts. This issue requires the utilisation of high laser powers [10], numerous scans per layer to cure the imperfections [11], and need further studies to gain optimised parameters.

The industrial concern for SLM parts from Aluminium combinations forces the topic of whether these parts will be dependable regarding mechanical properties. From a metallurgical viewpoint, using SLM process, Aluminium alloys creates a typically fine microstructure [12] created as a result of the quick rates of solidification. This may impact the mechanical properties when contrasted with coarse-grained material acquired through a conventional manufacturing process. The mechanical properties of SLM parts are influenced by several elements, for example, the build orientation [13]-[15], pre-heating of the build platform [16, 17], and the energy density conveyed to the material during processing [16].

The tensile behaviour [13, 16, 18, 19] and micro-hardness [14, 19] of SLM Aluminium parts with various degrees of porosity have been

beforehand explored indicating increased strength for the SLM material when contrasted with the conventional manufacturing process, in addition to reduced strength with expanded porosity.

The compressive behaviour of SLM Aluminium parts has, mainly, so far focussed on latticed structures [20] as opposed to solid parts. Previously, there are researchers that studied on the dimensional accuracy of SLM. Taib, et al. [21] found that samples with higher volume-to-surface area demonstrated the lower total amount of shrinkage as compared to lower volume-to-surface area. Through an experiment, they found that the increase in sample porosity leads to increase of shrinkage. For a better surface roughness, according to Qin and Chen [22], the roughness, Ra value, decreases with laser energy density increasing in one overlap ratio, while the overlap ratio is less than 50%.

In this paper, the authors attempt to determine the capability of SLM process in fabricating internally cooled tools using aluminium alloy (AlSi12), particularly the cooling channel, since it directly influences the cooling efficiency of the tool during a machining process. The channel manifold diameters were measured to determine the process accuracy, while surface roughness were used to determine the microstructure defects. The results of the cutting trials presented in this paper strongly suggested that the application of the ICCT will lead to substantial cost reductions and improvements in environmental conscious machining with the achievable tool life and surface roughness obtained.

## **Experimental Details**

### **Design ICCT**

A design of ICCT by [1, 23, 24] were constitutes of three (3) different main parts, which are the shank, the support and internal micro-channel. Table 1 shows the requirement and specification of those three (3) main parts of ICCT that need to be achieved such as surface roughness, shank width ( $w_s$ ), shank thickness ( $b_s$ ), channel width ( $w_c$ ), channel diameter ( $d_c$ ), and internal channel diameter ( $\phi_c$ ). The modelling process of ICCT was carried out by using CAD software, where all the dimensions were defined clearly in the three-dimensional (3D) model. Figure 1 depicts the 3D CAD model of ICCT without a cutting insert and a clamp bit that fixes the insert to the tool holder.

Table 1: Requirements and specifications of ICCT

Part	Requirement	Specification
Shank	<ul style="list-style-type: none"> <li>To be fixed firmly on the lathe machine.</li> </ul>	<ul style="list-style-type: none"> <li><math>w_s = 32</math> mm,</li> <li><math>b_s = 32</math> mm</li> <li>Tool steel material</li> </ul>
Support	<ul style="list-style-type: none"> <li>To supply the cooling fluid beneath cutting insert.</li> <li>To quickly remove the heat from cutting zone.</li> </ul>	<ul style="list-style-type: none"> <li>Flatness <math>&lt; 48</math> <math>\mu</math>m</li> <li>Surface Roughness, <math>R_a &lt; 20</math> <math>\mu</math>m</li> <li><math>w_c = 2</math> mm</li> <li><math>d_c = 2</math> mm</li> </ul>
micro-channel	<ul style="list-style-type: none"> <li>To supply laminar flow of coolant.</li> <li>To avoid back flow pressure.</li> </ul>	<ul style="list-style-type: none"> <li><math>\phi_c = 2</math> mm (internal)</li> <li>Attached to a pump through hose and nipple.</li> </ul>

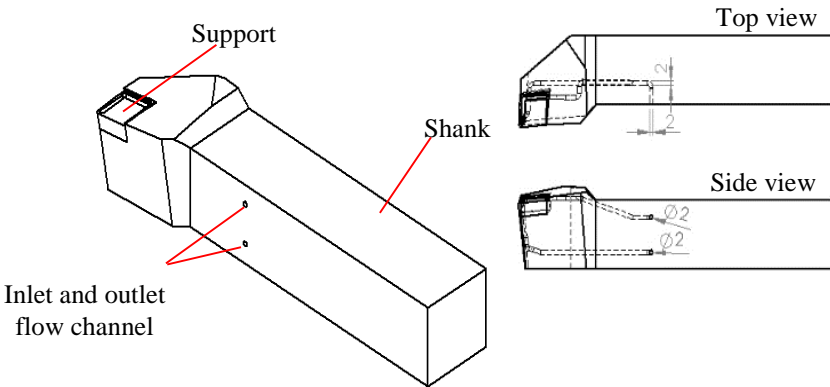


Figure 1: CAD drawing of ICCT (The units displayed are in mm)

### SLM Process

In the present experiment, an SLM system (SLM 280HL) was used. The process started by slicing the 3D CAD file data into layers of 100  $\mu$ m thick to produce a two-dimensional (2D) image of each layer and converted into a .stl file, which can be read by layer-based 3D printing technologies. This file was then loaded into a file preparation software package that assigns parameters, values and physical supports that allow the file to be interpreted and built by different types of additive manufacturing machines. Selective laser melting process commences with selectively melts thin layers of atomised fine metal powder are built onto a substrate plate that is fastened to

an indexing table that moves in the vertical (Z) axis as illustrated in Figure 2. This takes place inside a chamber containing a tightly controlled atmosphere of inert gas (argon) to prevent oxidation and contamination. Once powder layer has been distributed, each 2D slice of the part geometry is fused by selectively melting the powder. The SLM process parameters in this study are listed in Table 2, in which the parameters were recommended by the manufacturer. The process is repeated layer after layer until the part is complete.

Table 2: Process parameters of SLM machines

Parameters	Value
Laser power (W)	350
Hatching spacing (mm)	0.17
Scanning speed (mm/s)	930
Layer thickness ( $\mu\text{m}$ )	50
Chamber environment	Argon atmosphere

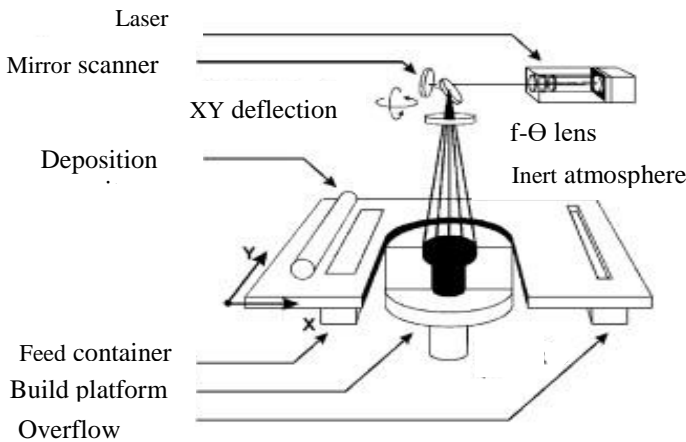


Figure 2: Schematic overview of SLM machine

### Dimensional measurement and density test

The measurement was conducted on several sections as shown in Figure 3, which is the diameter of the inlet and outlet of the channel, diameter of the internal channel at various locations (A, B, C, D, E, and F) and the arithmetic mean of surface roughness,  $R_a$ , randomly at (Top, Middle, and Bottom) sections. The measured dimensional data were then compared to the nominal value as per CAD design for obtaining build error data. In order to determine

surface roughness, the MarSurf PS1 perthometer device was used. The geometrical measurement was carried out using Dino-lite edge digital microscope modelled AM4815T and a digital calliper. The features of the digital microscope are 1.3 MP sensor resolution, adjustable focus and magnification from 20x up to 220x and provided with software measurement and calibration. The densities of the 6 samples were measured by applying Archimedes' principle. Relative density was calculated by the ratio of measured density to the theoretical density, as in Equation (1), where the theoretical density of AlSi12 is 2.7 g/cm<sup>3</sup>.

$$\text{Relative density (\%)} = \frac{\text{Measured density}}{\text{Theoretical density}} \quad (1)$$

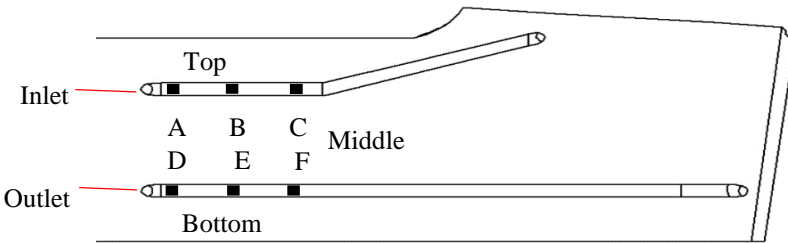


Figure 3: Half cut CAD drawing ICCT. Black spots in the channel are the points at where the measurements along are taken

### Compression test

All samples have been mechanically tested undertaking uniaxial compression testing. A universal testing machine (Instron 5985) was used to perform mechanical test. The parts were tested in different direction as illustrated in Figure 4 with 2 specimens per loading direction. The dimension of each specimen is (10 × 5 × 4.7) mm.

Compressive testing of the samples was performed by applying 50 kN force at constant deformation rate of 0.03 mm/s. The compressive strength and compressive strain (extension) were obtained from the stress-strain curve. In this study, the expected mechanical properties for the different direction indicated the anisotropic mechanical properties for the SLM produced samples.

All test were done under normal atmospheric conditions. Each static compression test resulted in a stress-strain curve. Strain was measured by the actual displacement of crossheads. The following values deviated from the compressive test where the elastic modulus as the slope of the compressive stress-strain curve in the linear region.

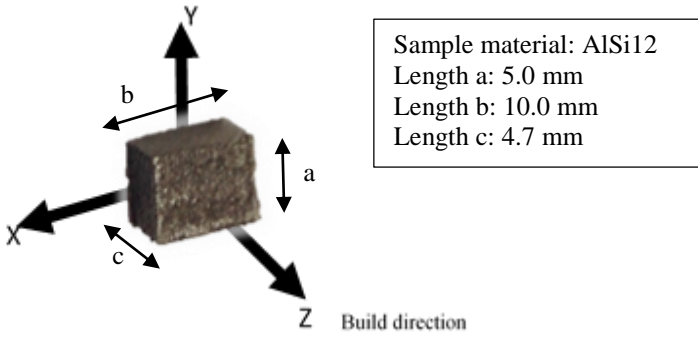


Figure 4: Direction of compression test

## Results and Discussion

### Relative density

Figure 5 shows the relative density of the selective laser melted for 6 samples of aluminium alloys. The average relative density is 99%. According to [25] the loss of density was observed due to porosities by the low-energy density, where the incomplete melting of the powder layer due to insufficient energy supply from laser irradiation. However, with the relative density of 99%, the SLM process used in this experiment is considered good compared to metal injection moulding (MIM) with a relative density of 97% [26].

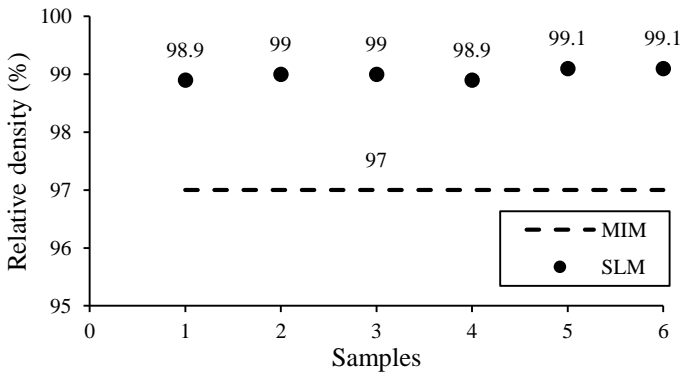


Figure 5 Relative density values of 6 samples SLM and density MIM

**Physical measurement**

A critical dimensional accuracy for ICCT is at the microchannel. The measured positions of microchannel were Inlet, Outlet, and Inlet/Outlet internal channel. The dimension for each position were measured using digital vernier calliper.

Table 3: Measured channel dimension of internally cooled tools

		CAD (mm)	SLM		
			$\bar{x}$	$s$	Error(%)
	Inlet	2	1.79	0.006	10.5
	Outlet	2	1.92	0.006	4
Inlet channel	A	2	1.92	0.006	4
	B	2	1.9	0.056	5
	C	2	1.9	0.012	5
Outlet channel	D	2	1.93	0.035	3.5
	E	2	1.91	0.026	4.5
	F	2	1.91	0.006	4.5
Mean Value :				0.019125	5.125

Table 3 shows the measured dimension of channel ICCT at various positions. The highest number of percentage error is acquired at Inlet with 10.5%. However, the other positions have errors of less than 5%. Thus, based on Fischer et al., the errors obtain in this experiment is within the tolerance of powder metallurgy, in which the SLM process is acceptable for ICCT fabrication [27].

**Surface roughness**

The surface roughness of a part is critical in many applications with some applications requiring very low surface roughness to avoid premature failure from surface initiated cracking [28].

Figure 6 shows the values of surface roughness measurement at different positions of ICCT. Although the position at the middle has high surface roughness compared to the top and bottom, but the standard deviation is the lowest. This is due to the thermal gradient that occurs during the SLM process that causes thermal expansion. The average surface roughness is 4.61  $\mu\text{m}$ . This value meets the requirement for internal channel condition of ICCT.

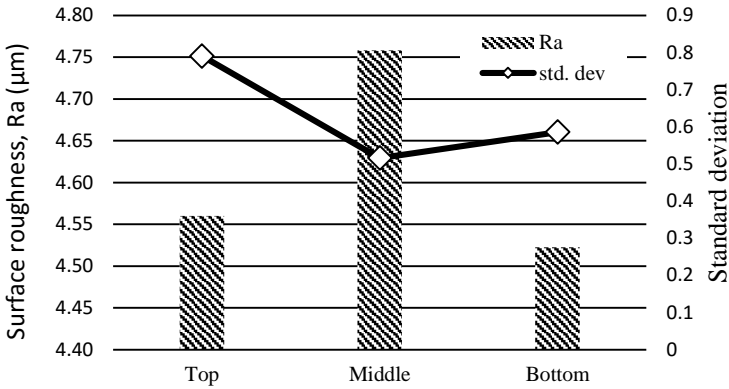


Figure 6: Surface roughness of ICCT

**Mechanical property**

Figure 7 clearly shows that the different direction of compression test has an isotropic relationship. Previously, Read, et al. [13] and Kempen, et al. [14] have reported on anisotropy in the mechanical properties of aluminium alloys. The agreement of the result above with the previous findings is quite revealing in several ways. Firstly, it indicates that thermal gradient plays significant effect during SLM process, which highlights the importance of optimum support design. Secondly, the result also reflects the effects attributed to process strategy, such as layer-to-layer thickness, the grain of powder structure and the scanning texture developed.

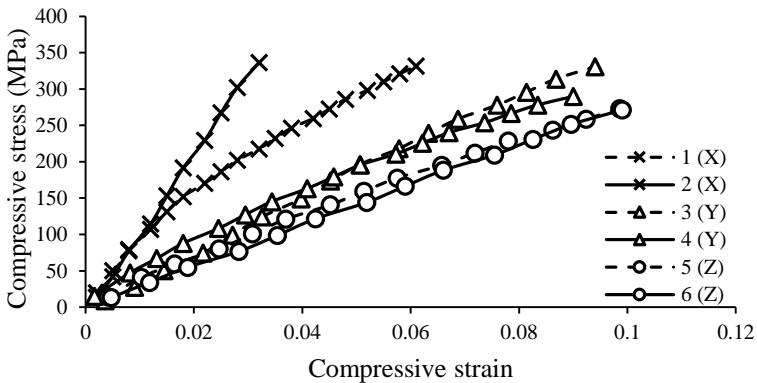


Figure 7 Stress-strain relationship for different compressive direction

## Preliminary Cutting Trials With SLM Manufactured ICCT

A series of cutting trials were carried out to investigate the practicality and effectiveness of this internally cooled cutting tool concept. The cutting trials were conducted on a CNC lathe (HAAS SL40). A customised 1 mm thickness uncoated cutting inserts was used and a steel adaptor was manufactured to hold inserts and prevent the cooling channel from leaking. The workpiece material was AISI 1017 mild steel in the form of a cylindrical rod (50 mm × 150 mm). The cutting parameters used were summarised as in Figure 9, where the depth of cut ( $a_p$ ), the feed rates ( $f$ ) and the cutting speed ( $V$ ) were set at 0.05 mm, 0.1 mm/rev, and 100 m/min respectively.

The progressive flank wear was measured by a portable optical microscope, as shown in Figure 8, after each cut. The cutting lengths vary from 5 to 10 minutes for each cut as demonstrated in Figure 9(a), whilst the surface roughness of the workpiece is depicted in Figure 9(b). The observation of the progressive flank wear and surface roughness indicate that the aluminium ICCT made by SLM can effectively perform cutting trials with acceptable useful tool life of over 60 minutes.

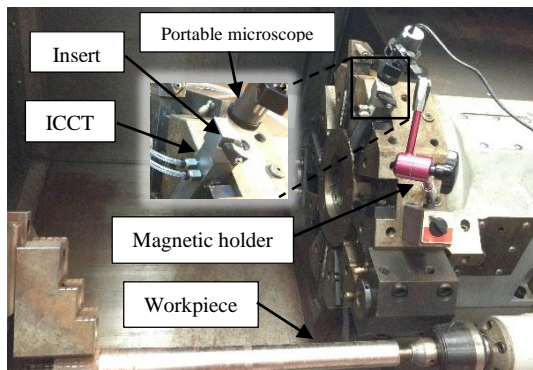
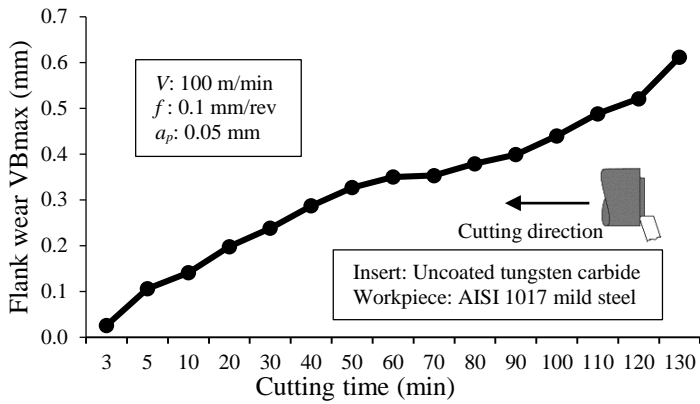
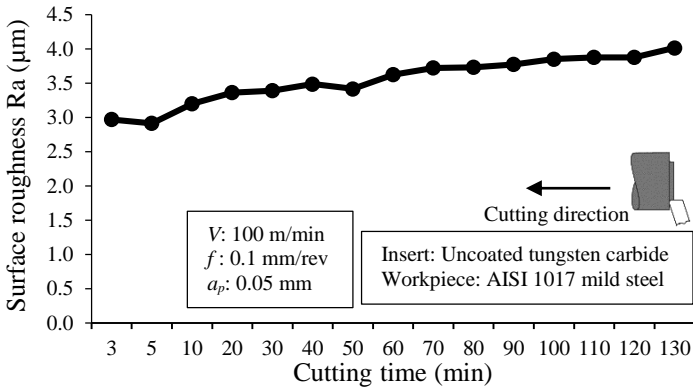


Figure 8 Experimental setup for flank wear measurement



(a)



(b)

Figure 9 (a) Maximum flank wear, and (b) surface roughness of finished workpiece

## Conclusion

Selective laser melting signify one of the additive manufacturing's greatest potential to attain a cleaner and more resource-efficient production in manufacturing. This study investigated the dimensional accuracy, density and compression strength of aluminium alloy (AlSi12) for potential use in manufacturing of internally cooled cutting tool using SLM process. The main findings of the work can be summarised as follows:

- The SLM process has high capability to manufacture ICCT with acceptable dimensional accuracy with 5.1% error. Most readings were under value to show the shrinkage.
- The recommended SLM parameters used in this work can produce ICCT with high relative density (99 %) and low surface roughness (4.61  $\mu\text{m}$ ). The results show minimum microstructure defects that encourages internal channel design.
- Stress-strain curve shows that the SLM process in this work has an isotropic relationship between a different direction of compression test. Further studies need to be done to achieve the isotropic relationship for ICCT fabrication. The closest mechanical property to the theoretical value of AISi12 is in the direction perpendicular to the direction of buildup.

## **Acknowledgements**

The authors are indebted to Mr Burhanuddin Noordin Ali, Dipl.-Ing. (FH) Muhd Izuddin Abdul Hamid and Mr Ad Azhar from Contraves Advance Devices Sdn. Bhd. for SLM processing and constructive discussions. This work has been supported by Universiti Malaysia Pahang under funded project RDU150338 and Malaysia Higher Education RACE grant RDU151313.

## **References**

- [1] X. Sun, R. Bateman, K. Cheng, and S. Ghani, "Design and analysis of an internally cooled smart cutting tool for dry cutting," Proceedings of the Institution of Mechanical Engineers, Part B: Journal of Engineering Manufacture, vol. 226, pp. 585-591, 2012.
- [2] E. Rahim, M. Ibrahim, A. Rahim, S. Aziz, and Z. Mohid, "Experimental investigation of minimum quantity lubrication (MQL) as a sustainable cooling technique," Procedia CIRP, vol. 26, pp. 351-354, 2015.
- [3] J. C. Rozzi, W. Chen, and E. E. Archibald, "Indirect cooling of a cutting tool," ed: Google Patents, 2011.
- [4] F. Wardle, T. Minton, S. B. C. Ghani, P. Frstmann, M. Roeder, S. Richarz, et al., "Artificial neural networks for controlling the temperature of internally cooled turning tools," 2013.
- [5] S. Che Ghani, K. Cheng, X. Z. Sun, and R. Bateman, "Optimizing Heat Transfer Rate in an Internally Cooled Cutting Tool: FE-Based Design Analysis and Experimental Study," in Key Engineering Materials, pp. 188-193, 2012.

- [6] C. Ferri, T. Minton, S. B. C. Ghani, and K. Cheng, "Efficiency in contamination-free machining using microfluidic structures," *CIRP Journal of Manufacturing Science and Technology*, vol. 7, pp. 97-105, 2014.
- [7] E. Wycisk, A. Solbach, S. Siddique, D. Herzog, F. Walther, and C. Emmelmann, "Effects of defects in laser additive manufactured Ti-6Al-4V on fatigue properties," *Physics Procedia*, vol. 56, pp. 371-378, 2014.
- [8] E. O. Olakanmi, R. F. Cochrane, and K. W. Dalgarno, "A review on selective laser sintering/melting (SLS/SLM) of aluminium alloy powders: Processing, microstructure, and properties," *Progress in Materials Science*, vol. 74, pp. 401-477, 10// 2015.
- [9] V. Matilainen, H. Piili, A. Salminen, T. Syvänen, and O. Nyrhilä, "Characterization of process efficiency improvement in laser additive manufacturing," *Physics Procedia*, vol. 56, pp. 317-326, 2014.
- [10] D. Buchbinder, H. Schleifenbaum, S. Heidrich, W. Meiners, and J. Bültmann, "High power selective laser melting (HP SLM) of aluminum parts," *Physics Procedia*, vol. 12, pp. 271-278, 2011.
- [11] N. T. Aboulkhair, N. M. Everitt, I. Ashcroft, and C. Tuck, "Reducing porosity in AlSi10Mg parts processed by selective laser melting," *Additive Manufacturing*, vol. 1, pp. 77-86, 2014.
- [12] L. Thijs, K. Kempen, J.-P. Kruth, and J. Van Humbeeck, "Fine-structured aluminium products with controllable texture by selective laser melting of pre-alloyed AlSi10Mg powder," *Acta Materialia*, vol. 61, pp. 1809-1819, 2013.
- [13] N. Read, W. Wang, K. Essa, and M. M. Attallah, "Selective laser melting of AlSi10Mg alloy: Process optimisation and mechanical properties development," *Materials & Design*, vol. 65, pp. 417-424, 2015.
- [14] K. Kempen, L. Thijs, J. Van Humbeeck, and J.-P. Kruth, "Mechanical properties of AlSi10Mg produced by selective laser melting," *Physics Procedia*, vol. 39, pp. 439-446, 2012.
- [15] M. Simonelli, Y. Tse, and C. Tuck, "Effect of the build orientation on the Mechanical Properties and Fracture Modes of SLM Ti-6Al-4V," *Materials Science and Engineering: A*, vol. 616, pp. 1-11, 2014.
- [16] S. Siddique, M. Imran, E. Wycisk, C. Emmelmann, and F. Walther, "Influence of process-induced microstructure and imperfections on mechanical properties of AlSi12 processed by selective laser melting," *Journal of Materials Processing Technology*, vol. 221, pp. 205-213, 2015.
- [17] E. Brandl, U. Heckenberger, V. Holzinger, and D. Buchbinder, "Additive manufactured AlSi10Mg samples using Selective Laser

- Melting (SLM): Microstructure, high cycle fatigue, and fracture behavior," *Materials & Design*, vol. 34, pp. 159-169, 2012.
- [18] K. Prashanth, S. Scudino, H. Klauss, K. B. Surreddi, L. Löber, Z. Wang, et al., "Microstructure and mechanical properties of Al–12Si produced by selective laser melting: Effect of heat treatment," *Materials Science and Engineering: A*, vol. 590, pp. 153-160, 2014.
- [19] X. Wang, L. Zhang, M. Fang, and T. B. Sercombe, "The effect of atmosphere on the structure and properties of a selective laser melted Al–12Si alloy," *Materials Science and Engineering: A*, vol. 597, pp. 370-375, 2014.
- [20] C. Qiu, S. Yue, N. J. Adkins, M. Ward, H. Hassanin, P. D. Lee, et al., "Influence of processing conditions on strut structure and compressive properties of cellular lattice structures fabricated by selective laser melting," *Materials Science and Engineering: A*, vol. 628, pp. 188-197, 2015.
- [21] Z. A. M. Taib, W. S. W. Harun, S. A. C. Ghani, M. F. F. A. Rashid, M. A. Omar, and H. Ramli, "Dimensional Accuracy Study of Open Cellular Structure CoCrMo Alloy Fabricated by Selective Laser Melting Process," *Advanced Materials Research*, vol. 1133, 2016.
- [22] Q. Qin and G. X. Chen, "Effects of Parameters on Surface Roughness of Metal Parts by Selective Laser Melting," in *Advanced Materials Research*, pp. 872-875, 2014.
- [23] R. H. Kraemer, "Tool holder with coolant system," ed: Google Patents, 2003.
- [24] Y. Isik, "Using internally cooled cutting tools in the machining of difficult-to-cut materials based on Waspaloy," *Advances in Mechanical Engineering*, vol. 8, pp. 1-8, 2016.
- [25] T. Kimura and T. Nakamoto, "Microstructures and mechanical properties of A356 (AlSi7Mg0.3) aluminum alloy fabricated by selective laser melting," *Materials & Design*, vol. 89, pp. 1294-1301, 1/5/2016.
- [26] Z. Liu, T. Sercombe, and G. Schaffer, "Metal injection moulding of aluminium alloy 6061 with tin," *Powder Metallurgy*, vol. 51, pp. 78-83, 2008.
- [27] U. Fischer, M. Heinzler, and K. Eberscheg, *Tabellenbuch Metall: Verlag Europa-Lehrmittel Nourney, Vollmer*, 2008.
- [28] K. Dalgarno, "Materials research to support high performance RM parts," in *Rapid Manufacturing 2nd International Conference*, Loughborough University, pp. 9-12, 2007.